

# Application of the Method of Maximum Likelihood to Identification of Bipedal Walking Robots

Kamil Dolinský and Sergej Čelikovský

**Abstract**—This brief studies the problem of parameter estimation and model identification for a class of underactuated mechanical systems modeled via the Euler–Lagrange formalism, such as underactuated walking robots. This problem is closely related with the measurement of the absolute orientation during walking. A novel identification method suited for this problem was proposed. The method takes advantage of the linear structure of the model with respect to estimated parameters. The resulting estimator is calculated iteratively and maximizes the likelihood of the data. The method was tested on both simulated and experimental data. Simulation was carried out for an underactuated walking robot with a distance meter to measure absolute orientation. Laboratory experiment was carried out on a leg of a laboratory walking robot model equipped with a three-axis accelerometer and gyroscope to measure absolute orientation. The method performs favorably in comparison with other benchmark estimation algorithms and both the simulation example and the laboratory experiment confirmed its high potential for the use in identification of underactuated robotic walkers.

**Index Terms**—Control, identification, maximum likelihood (ML), walking robots.

## I. INTRODUCTION

UNDERACTUATED walking robots have been studied intensively in recent decades. And many results connected to model-based nonlinear control algorithms were developed [10], [19]. A mathematical model of the robot—a mechanical chain of rigid links—can be obtained using classical mechanics, for example via Euler–Lagrange formalism [11]. This brief deals with experimental identification of such systems—that is estimating the mathematical model from data provided by robot’s sensors [12], [16]. The main benefit of such approach is that the model can be improved by using the data from walking. Although kinematic parameters such as lengths of robot’s legs or thighs can be measured directly, the values of parameters related to dynamic behavior of robot—location of center of gravity, inertia, and friction effects—are more difficult to obtain, especially if

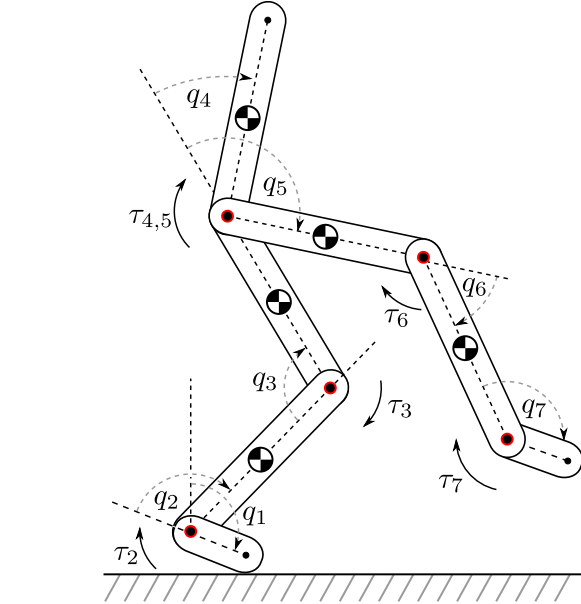


Fig. 1. Schematics of the mechanical chain representing a walking robot.

the robot is more complicated. Other uses include mechanical changes in the robot, in such an event experimental identification can be very valuable. The underactuation is a fundamental problem of robotic walking, since it is present in any agile humanoid walking robot. It means that the system has more degrees of freedom than independent actuators [19]. The underactuation occurs whenever the foot of the robot is not flat on the ground. This is because the contact point between the foot and the ground can be modeled as a pivot point. However, this pivot point is not directly actuated and it is not possible to place a motor to actuate robot in that point (see Fig. 1) and note the underactuated angle  $q_1$ . All the remaining joints of the robot can be actuated directly using motors. This fact is closely related to the problem of model identification. To identify a model of an underactuated walking robot from measurements obtained during walking, an information about the absolute orientation of the robot is required. It is possible to measure all the relative angles between the links of robot using optical encoders or encoders based on Hall effect. These provide accurate information about relative angles between the links of the robot. Furthermore, these measurements can be used to obtain information about relative angular velocities and accelerations between links. However, due to the underactuation, it is not possible to use an encoder to directly measure the absolute orientation of a walking robot. This information has to be obtained using different sensors. The human sensory system relies mostly on the sight and the inner ear. This brief, therefore, studies two concepts of the absolute

Manuscript received February 27, 2017; accepted April 25, 2017. Date of publication June 20, 2017; date of current version June 11, 2018. Manuscript received in final form May 21, 2017. This work was supported by the Czech Science Foundation under Grant 17-04682S. Recommended by Associate Editor H. Wang. (Corresponding author: Kamil Dolinský.)

K. Dolinský is with the Institute of Information Theory and Automation, Czech Academy of Sciences, 182 08 Prague, Czech Republic, and also with the Faculty of Electrical Engineering, Czech Technical University in Prague, 121 35 Prague, Czech Republic (e-mail: kamil.dolinsky@fel.cvut.cz).

S. Čelikovský is with the Institute of Information Theory and Automation, Czech Academy of Sciences, 182 08 Prague, Czech Republic (e-mail: celikovs@utia.cas.cz).

Color versions of one or more of the figures in this paper are available online at <http://ieeexplore.ieee.org>.

Digital Object Identifier 10.1109/TCST.2017.2709277

orientation measurement, the first uses a visual feedback providing the distance of the robot to a point on the ground. The second concept uses a gyroscope and an accelerometer. Such an unavailability of the absolute orientation measurements is the main difference, which distinguishes the problem of identifying the model of walking robot from a closely related problem of identification of robotic manipulators [2]–[5], [7]–[9]. For both, walking robots and manipulator robots, joint torques are related only with configuration angles, angular velocities, angular accelerations, and parameters. When the appropriate parameterization of model is used, this relationship is linear in parameters. In the case when the angular data are available and are accurate, they can be used to construct regression matrix for this estimation problem and the method of weighted least squares (WLS) can be used to estimate the parameters [1]. A robotic manipulator is a fully actuated mechanical chain, and therefore, all of the configuration angles—including the absolute orientation angle—can be accurately measured using encoders. Associated angular velocities and accelerations can be estimated using filtered finite differences. On the contrary, the underactuation of walking robots resulting in the unavailability of encoder readings of the absolute orientation angle and the necessity of measuring the angle using sensors susceptible to errors complicates the estimation procedure. This brief studies two issues: first, how to include the information about the absolute orientation into the estimation procedure when the angle is not directly measured and second, how to remove the errors from the absolute orientation data, using the maximum likelihood estimation (MLE) method, so that the assumptions of the WLS estimator are not violated. These issues are studied on two examples. The first example is a simulation study of a three link walking robot, which uses a laser distance measurement to measure the underactuated angle. This example shows that the approach developed in this brief can deal with the measurement errors and performs favorably in comparison with other common estimation methods. The other example is a laboratory experiment, where the parameters of a leg of an underactuated walking robot are estimated and the underactuated angle is measured using a three-axis accelerometer and gyroscope LSM9DS1 [22].

## II. STRUCTURE OF IDENTIFIED SYSTEMS

An open kinematic chain consisting of  $n_r$  links is a mechanical system of  $n_r$  degrees of freedom and its motion can be described by  $n_r - 1$  relative angles  $q_i^r$  and corresponding  $n_r - 1$  angular velocities  $\dot{q}_i^r$  and one absolute angle  $q^a$  and its associated velocity  $\dot{q}^a$ . All these angles at a particular time  $t$  form a vector of configuration angles  $\mathbf{q}(t)$  and together with the vector of angular velocities  $\dot{\mathbf{q}}(t)$  they constitute the state vector  $\mathbf{x}(t)$ . Torques corresponding to each degree of freedom are included in the vector  $\boldsymbol{\tau}(t)$  and vector  $\mathbf{u}(t)$  comprises the actuator torques. Summarizing

$$\mathbf{q}(t) = [q_1^r(t), \dots, q_{n_r-1}^r(t), q^a(t)]^T = [\mathbf{q}^r(t), q^a(t)]^T \quad (1)$$

$$\dot{\mathbf{q}}(t) = [\dot{q}_1^r(t), \dots, \dot{q}_{n_r-1}^r(t), \dot{q}^a(t)]^T = [\dot{\mathbf{q}}^r(t), \dot{q}^a(t)]^T \quad (2)$$

$$\mathbf{x}(t) = [\mathbf{q}^T(t), \dot{\mathbf{q}}^T(t)]^T \quad (3)$$

$$\boldsymbol{\tau}(t) = [\tau_1(t), \dots, \tau_{n_r}(t)]^T \quad (4)$$

$$\mathbf{u}(t) = [u_1(t), \dots, u_{n_r-1}(t)]^T. \quad (5)$$

Kinematic chains can be modeled by Euler–Lagrange’s equations of motion

$$\frac{d}{dt} \left( \frac{\partial \mathcal{L}}{\partial \dot{\mathbf{q}}} \right) - \frac{\partial \mathcal{L}}{\partial \mathbf{q}} = \boldsymbol{\tau} \quad (6)$$

where  $\mathcal{L}$  denotes the Lagrangian, which equals the difference between the kinetic and the potential energy of considered mechanical system, that is

$$\mathcal{L} = K(\mathbf{q}, \dot{\mathbf{q}}) - V(\mathbf{q}). \quad (7)$$

The kinetic energy of the system is given as

$$K(\mathbf{q}, \dot{\mathbf{q}}) = \frac{1}{2} \dot{\mathbf{q}}^T \mathbf{D}(\mathbf{q}) \dot{\mathbf{q}}, \quad \mathbf{D}(\mathbf{q}) = \mathbf{D}^T(\mathbf{q}) \succ 0 \quad (8)$$

and (6) will assume the following form [19]:

$$\mathbf{B}\mathbf{u} = \boldsymbol{\tau} = \mathbf{D}(\mathbf{q})\ddot{\mathbf{q}} + \mathbf{C}(\mathbf{q}, \dot{\mathbf{q}})\dot{\mathbf{q}} + \mathbf{G}(\mathbf{q}) + \mathbf{F}(\mathbf{q}, \dot{\mathbf{q}}) \quad (9)$$

$$\mathbf{G}(\mathbf{q}) = \frac{\partial V(\mathbf{q})}{\partial \mathbf{q}} \quad (10)$$

$$\mathbf{C}(\mathbf{q}, \dot{\mathbf{q}}) = \frac{\partial}{\partial \mathbf{q}} (\mathbf{D}(\mathbf{q})\dot{\mathbf{q}}) - \frac{1}{2} \left( \frac{\partial}{\partial \mathbf{q}} (\mathbf{D}(\mathbf{q})\dot{\mathbf{q}}) \right)^T. \quad (11)$$

Matrix  $\mathbf{D}(\mathbf{q})$  is called the inertia matrix,  $\mathbf{C}(\mathbf{q}, \dot{\mathbf{q}})$  is the matrix of Coriolis and centrifugal forces, and vector  $\mathbf{G}(\mathbf{q})$  describes gravity effects and vector  $\mathbf{F}(\mathbf{q}, \dot{\mathbf{q}})$  contains friction model terms. Matrix  $\mathbf{B}$  describes how the actuator torques  $\mathbf{u}$  are generating torques  $\boldsymbol{\tau}$ . The associated state space model can be found using (3) and (9) as

$$\dot{\mathbf{x}} = \mathbf{f}(\mathbf{x}) + \mathbf{g}(\mathbf{x})\mathbf{u}. \quad (12)$$

## III. PARAMETER ESTIMATION

Using link masses, inertia tensors, link lengths, and so on, to parameterize the motion equations of a mechanical chain is quite natural. For the purpose of parameter estimation it is, however, more advantageous to use a parameterization that allows a model linear in parameters

$$\mathbf{B}\mathbf{u}(t) = \boldsymbol{\tau}(t) = \mathbf{Z}(\mathbf{q}(t), \dot{\mathbf{q}}(t), \ddot{\mathbf{q}}(t))\boldsymbol{\beta} \quad (13)$$

where the matrix  $\mathbf{Z}(\mathbf{q}(t), \dot{\mathbf{q}}(t), \ddot{\mathbf{q}}(t))$  can be formed by manipulating the left-hand side of (9). The structural identifiability of parameters  $\boldsymbol{\beta}$  can be easily ensured by choosing a parameterization that makes the corresponding matrix  $\mathbf{Z}$  of full rank. To be able to exploit the linearity in the parameters, all variables entering the design matrix  $\mathbf{Z}$  must be available. Then, the problem of parameter estimation reduces to a problem of multivariate linear regression [1], [17], [18], [20], [21].

### A. Estimating Relative Angular Velocities and Accelerations

A typical situation encountered in practice is that the measurements of actuator torques and relative angles are available from motor-current sensors and rotary encoders, respectively. The encoder data are usually very accurate, and after digital filtering, practically noise free. For data set consisting of  $N$  samples, we have

$$\mathbf{y}_\tau(t_k) = \boldsymbol{\tau}(t_k) + \mathbf{e}_\tau(t_k) = \mathbf{B}\mathbf{y}_u(t_k) \quad (14)$$

$$\mathbf{y}_u(t_k) = \mathbf{u}(t_k) + \mathbf{e}_u(t_k) \quad (15)$$

$$\mathbf{y}_q(t_k) \approx \mathbf{q}^r(t_k) \quad (16)$$

where  $k = 1 \dots N$ . Actuator-torques measurement errors  $\mathbf{e}_u(t_k)$  are assumed to be independent, identically distributed, following normal distribution and to have zero mean. That is

$$\mathbb{E}[\mathbf{e}_u(t_k)\mathbf{e}_u(t_k)^T] = \mathbf{\Sigma}_u \quad (17)$$

$$\mathbb{E}[\mathbf{e}_u(t_k)\mathbf{e}_u(t_l)^T] = 0 \quad \text{for } t_l \neq t_k. \quad (18)$$

As a consequence,  $\mathbf{e}_\tau \sim \mathcal{N}(0, \mathbf{\Sigma}_\tau)$ , where  $\mathbf{\Sigma}_\tau = \mathbf{B}\mathbf{\Sigma}_u\mathbf{B}^T$ . On the other hand, the angular velocities and accelerations are usually not available, but in the case of relative angles, they can be estimated from angular data using central differences

$$\hat{\mathbf{q}}_{\text{fcd}}^r(t_k) = \frac{\hat{\mathbf{q}}_f^r(t_k + T_s) - \hat{\mathbf{q}}_f^r(t_k - T_s)}{2T_s} \quad (19)$$

$$\hat{\mathbf{q}}_{\text{fcd}}^a(t_k) = \frac{\hat{\mathbf{q}}_f^r(t_k + 2T_s) - 2\hat{\mathbf{q}}_f^r(t_k) + \hat{\mathbf{q}}_f^r(t_k - 2T_s)}{4T_s^2} \quad (20)$$

where  $\hat{\mathbf{q}}_f^r$  denotes digitally filtered relative angular data,  $T_s$  the sampling rate and the filtering is used to reduce the noise amplification introduced by numerical differences.

### B. Eliminating the Dependence on the Absolute Angle

There are various sensors that can measure various quantities  $\mathbf{h}$  that are directly related to the absolute angle, e.g., distance from the ground or linear accelerations measured by an accelerometer. These quantities can be used to eliminate  $\mathbf{q}^a$  from (13). To achieve this using accelerometer measurements, both  $\dot{\mathbf{q}}^a$  and  $\ddot{\mathbf{q}}^a$  are required. Angular velocity  $\dot{\mathbf{q}}^a$  can be measured using gyroscope and  $\ddot{\mathbf{q}}^a$  can be obtained using central differences from filtered measurements of  $\dot{\mathbf{q}}^a$ . Therefore, the following measurement model is obtained:

$$\mathbf{y}_h(t_k) = \mathbf{h}(t_k) + \mathbf{e}_h(t_k) \quad (21)$$

$$\mathbf{y}_{\dot{\mathbf{q}}^a}(t_k) = \dot{\mathbf{q}}^a(t_k) + \mathbf{e}_{\dot{\mathbf{q}}^a}(t_k). \quad (22)$$

For a compact reference, the following vectors are defined for the case of accelerometer measurements:

$$\mathbf{y}_a(t_s) = [\mathbf{y}_h(t_k), \mathbf{y}_{\dot{\mathbf{q}}^a}(t_k)]^T \quad (23)$$

$$\mathbf{e}_a(t_s) = [\mathbf{e}_h(t_k), \mathbf{e}_{\dot{\mathbf{q}}^a}(t_k)]^T \quad (24)$$

where  $\mathbf{e}_a(t_k) \sim \mathcal{N}(0, \mathbf{\Sigma}_a)$ . And the vector  $\mathbf{y}_a(t_s) = \mathbf{y}_h(t_k)$  in the case of distance meter and it is assumed that associated changes can be carried out by the reader. Measurement errors  $\mathbf{e} = [\mathbf{e}_\tau^T, \mathbf{e}_a^T]^T$  are assumed to be normally distributed with zero mean and to be uncorrelated across time. Thus

$$\mathbb{E}[\mathbf{e}(t_k)\mathbf{e}(t_k)^T] = \mathbf{\Sigma} = \begin{bmatrix} \mathbf{\Sigma}_\tau & 0 \\ 0 & \mathbf{\Sigma}_a \end{bmatrix} \quad (25)$$

$$\mathbb{E}[\mathbf{e}(t_k)\mathbf{e}(t_l)^T] = 0 \quad \text{for } t_l \neq t_k. \quad (26)$$

The covariance of errors  $\mathbf{e}_h(t_k)$  is either constant or dependent on the quantity  $\mathbf{h}(t_k)$ , a typical example is when the error of the distance measurement grows with the distance. The model for a whole data set can be written as

$$\mathbf{y}_{\tau,1\dots N} = \tilde{\mathbf{Z}}_{1\dots N}(\hat{\mathbf{h}}_f, \hat{\mathbf{q}}_f^r, \hat{\mathbf{q}}_f^a, \hat{\mathbf{q}}_f^a)\boldsymbol{\beta} + \mathbf{e}_{\tau,1\dots N} + \mathbf{v}_{1\dots N} \quad (27)$$

where  $\hat{\mathbf{q}}_f = [\hat{\mathbf{q}}_{\text{fcd}}^r, \hat{\mathbf{q}}_f^a]^T$ ,  $\hat{\mathbf{q}}_f^a = [\hat{\mathbf{q}}_{\text{fcd}}^r, \hat{\mathbf{q}}_{\text{fcd}}^a]^T$ , where  $\hat{\mathbf{q}}^a$  is either calculated from distance measurements using finite differences, or determined by the gyroscope measurements  $\mathbf{y}_{\dot{\mathbf{q}}^a}$ ,  $\hat{\mathbf{q}}_{\text{fcd}}^a$

is a central difference-based estimate of  $\ddot{\mathbf{q}}^a$  calculated from  $\hat{\mathbf{q}}^a$ . The matrix  $\tilde{\mathbf{Z}}$  equals matrix  $\mathbf{Z}$ , but is now parametrized using the filtered measurements  $\hat{\mathbf{h}}_f$  of the quantities  $\mathbf{h}$ , which are measurable—contrary to the absolute angle  $\mathbf{q}^a$ . Error  $\mathbf{v}$  stands for errors due to unmodeled dynamics or discrepancies in the design matrix caused by angular measurement errors. Since the structure of the identified system can be described accurately by the Euler–Lagrange equations, it is assumed that the errors due to unmodeled dynamics can be neglected. If there are any additional dynamic phenomena, such as friction or gear dynamics, they should be included in the model. In the case when the positional data are accurate, the discrepancies in the design matrix as well as potential correlation due to closed loop can both be neglected (see [5], [14], [15] and references therein). In such a case,  $\boldsymbol{\beta}$  can be estimated using the WLS estimator

$$\hat{\boldsymbol{\beta}} = (\tilde{\mathbf{Z}}_{1\dots N}^T \mathbf{W} \tilde{\mathbf{Z}}_{1\dots N})^{-1} (\tilde{\mathbf{Z}}_{1\dots N}^T \mathbf{W} \mathbf{y}_{1\dots N}) \quad (28)$$

where the weighting matrix is equal to

$$\mathbf{W} = \mathbf{\Sigma}_\tau \otimes \mathbf{1}_{N \times N}. \quad (29)$$

However, this method does not explicitly account for the measurement noise in the absolute orientation data and, therefore, cannot provide optimal estimates when measurements are noisy—which is the case of walking robots.

## IV. MAXIMUM LIKELIHOOD ESTIMATION OF PARAMETERS FROM OPEN-LOOP NOISY DATA

Due to errors in the measurements determining the absolute orientation of the robot, the design matrix

$$\tilde{\mathbf{Z}}(\hat{\mathbf{h}}_f, \hat{\mathbf{q}}_f^r, \hat{\mathbf{q}}_f^a, \hat{\mathbf{q}}_f^a) \neq \tilde{\mathbf{Z}}(\mathbf{h}, \mathbf{q}^r, \dot{\mathbf{q}}, \ddot{\mathbf{q}}) \quad (30)$$

and the resulting estimate of parameters will be biased. Therefore, one would like to find estimates of  $\hat{\mathbf{h}}_{\text{mle}}(t_k)$ ,  $\hat{\mathbf{q}}_{\text{mle}}^a(t_k)$  and  $\hat{\mathbf{q}}_{\text{mle}}^a(t_k)$ , which most likely correspond to the values of  $\mathbf{h}(t_k)$ ,  $\dot{\mathbf{q}}^a(t_k)$  and  $\ddot{\mathbf{q}}^a(t_k)$ , respectively, for  $k = 1, \dots, N$ . It is assumed that the error properties (25) are known. To be more specific, matrix  $\mathbf{\Sigma}$ , or matrices  $\mathbf{\Sigma}_\tau$  and  $\mathbf{\Sigma}_a$ , are known up to a scalar multiple. Estimates of these matrices can be obtained from specially designed repeated experiments. The distribution of measurements  $\mathbf{y}_\tau(t_k)$  and  $\mathbf{y}_a(t_k)$  is given by multivariate normal distribution

$$f(\mathbf{y}_\tau(t_k), \mathbf{y}_a(t_k)) = \frac{1}{\sqrt{(2\pi)^{2r} |\mathbf{\Sigma}|}} \exp\left(-\frac{1}{2} \mathbf{e}(t_k)^T \mathbf{\Sigma}^{-1} \mathbf{e}(t_k)\right). \quad (31)$$

The likelihood function of measurements  $\mathbf{y}_\tau(t_k)$  and  $\mathbf{y}_a(t_k)$  is a function of  $\boldsymbol{\tau}(t_k)$  and  $\mathbf{h}(t_k)$ ,  $\dot{\mathbf{q}}^a(t_k)$ ,  $\ddot{\mathbf{q}}^a(t_k)$  and is proportional to (31). By using the model (27), estimator (28), and by using central differences to eliminate all the derivatives, one concludes that  $\ell$  for a whole data set is given as

$$\ell(\mathbf{h}_{1\dots N}, \dot{\mathbf{q}}_{1\dots N}^a) = \prod_{k=1}^{k=N} \exp\left(-\frac{1}{2} \mathbf{e}(t_k)^T \mathbf{\Sigma}^{-1} \mathbf{e}(t_k)\right). \quad (32)$$

Maximization of  $\ell(\mathbf{h}_{1\dots N}, \dot{\mathbf{q}}_{1\dots N}^a)$  can be obviously achieved by minimizing the sum of squares

$$S(\mathbf{h}_{1\dots N}, \dot{\mathbf{q}}_{1\dots N}^a) = \sum_{k=1}^{k=N} (\mathbf{e}(t_k)^T \boldsymbol{\Sigma}^{-1} \mathbf{e}(t_k)). \quad (33)$$

#### A. Implementation of the Minimization Procedure

Minimizing the criterion (33) is a nonconvex optimization problem and, therefore, the solution has to be sought iteratively. However, the sum of squares can be calculated extremely efficiently thanks to utilizing the WLS estimator in conjunction with the central differences. In particular, this approach does not require to integrate the equations of motion. The implementation of the identification procedure can be performed using the following steps, with some small differences, which depend on whether the absolute orientation was measured using the distance meter or using the combination of accelerometers and gyroscopes.

##### 1) Initialization:

- a) Set the iteration counter to  $i = 1$ .
- b) For  $k = 1 \dots N$ , filter the actuator torques, relative angles, the quantity  $\mathbf{h}$  related to the absolute angle

$$\hat{\mathbf{u}}_f(t_k) = \text{lowpass}(\mathbf{y}_u(t_k)) \quad (34)$$

$$\hat{\mathbf{q}}_f^r(t_k) = \text{lowpass}(\mathbf{y}_q^r(t_k)) \quad (35)$$

$$\hat{\mathbf{h}}_f(t_k) = \text{lowpass}(\mathbf{y}_h(t_k)). \quad (36)$$

If accelerometers and gyroscopes are used then also filter the gyroscope measurements

$$\hat{\mathbf{q}}_f^a(t_k) = \text{lowpass}(\mathbf{y}_{\dot{q}}^a(t_k)). \quad (37)$$

- c) For  $k = 1 \dots N$ , calculate finite difference-based estimates

$$\hat{\mathbf{q}}_{\text{fcd}}^r(t_k) = \frac{\hat{\mathbf{q}}_f^r(t_k + T_s) - \hat{\mathbf{q}}_f^r(t_k - T_s)}{2T_s} \quad (38)$$

$$\hat{\mathbf{q}}_{\text{fcd}}^a(t_k) = \frac{\hat{\mathbf{q}}_{\text{fcd}}^r(t_k + T_s) - \hat{\mathbf{q}}_{\text{fcd}}^r(t_k - T_s)}{2T_s}. \quad (39)$$

- d) For  $k = 1 \dots N$  calculate  $\mathbf{y}_\tau(t_k) = \mathbf{B}\hat{\mathbf{u}}_f(t_k)$  and form the vector  $\mathbf{y}_{\tau,1\dots N}$ .
- e) Initialize the ML estimator of absolute orientation data as

$$\hat{\mathbf{h}}_{\text{mle},1}(t_k) = \hat{\mathbf{h}}_f(t_k) \quad (40)$$

and in the case of accelerometers and gyroscopes also

$$\hat{\mathbf{q}}_{\text{mle},1}^a(t_k) = \hat{\mathbf{q}}_f^a(t_k). \quad (41)$$

##### 2) Calculation of Minimization Criterion:

- a) In the case of distance meter, estimate the angle  $\hat{\mathbf{q}}_{\text{mle}}^a(t_k)$  using the estimate  $\hat{\mathbf{h}}_{\text{mle},i}(t_k)$  and for  $k = 1 \dots N$  calculate

$$\hat{\mathbf{q}}_{\text{mle},i}^a(t_k) = \frac{\hat{\mathbf{q}}_{\text{mle},i}^a(t_k + T_s) - \hat{\mathbf{q}}_{\text{mle},i}^a(t_k - T_s)}{2T_s}. \quad (42)$$

In the case of accelerometers and gyroscopes, this step is omitted.

- b) For  $k = 1 \dots N$ , calculate the central differences-based estimate from the current ML estimate  $\hat{\mathbf{q}}_{\text{mle},i}^a(t_k)$  as

$$\hat{\mathbf{q}}_{\text{mle},i}^a(t_k) = \frac{\hat{\mathbf{q}}_{\text{mle},i}^a(t_k + T_s) - \hat{\mathbf{q}}_{\text{mle},i}^a(t_k - T_s)}{2T_s}. \quad (43)$$

- c) Form the design matrix  $\tilde{\mathbf{Z}}$  for each  $k = 1 \dots N$  as

$$\tilde{\mathbf{Z}}(t_k) = \tilde{\mathbf{Z}}(\hat{\mathbf{h}}_{\text{mle},i}(t_k), \hat{\mathbf{q}}_{\text{mle},i}^a(t_k), \hat{\mathbf{q}}_{\text{mle},i}^a(t_k), \hat{\mathbf{q}}^r(t_k), \hat{\mathbf{q}}^r(t_k), \hat{\mathbf{q}}^r(t_k)). \quad (44)$$

- d) Form matrices  $\tilde{\mathbf{Z}}_{1\dots N}$  and  $\mathbf{W}$  and calculate the estimate of parameters as

$$\hat{\boldsymbol{\beta}} = (\tilde{\mathbf{Z}}_{1\dots N}^T \mathbf{W} \tilde{\mathbf{Z}}_{1\dots N})^{-1} (\tilde{\mathbf{Z}}_{1\dots N}^T \mathbf{W} \mathbf{y}_{\tau,1\dots N}). \quad (45)$$

- e) For  $k = 1 \dots N$ , calculate the joint torques predicted by the ML estimates

$$\boldsymbol{\tau}_{\text{mle},i}(t_k) = \tilde{\mathbf{Z}}(\hat{\mathbf{h}}_{\text{mle},i}(t_k), \hat{\mathbf{q}}_{\text{mle},i}^a(t_k), \hat{\mathbf{q}}_{\text{mle},i}^a(t_k), \hat{\mathbf{q}}^r(t_k), \hat{\mathbf{q}}^r(t_k), \hat{\mathbf{q}}^r(t_k)) \boldsymbol{\beta}. \quad (46)$$

- f) For  $k = 1 \dots N$ , calculate residuals

$$\mathbf{e}_\tau(t_k) = \mathbf{y}_\tau(t_k) - \boldsymbol{\tau}_{\text{mle},i}(t_k) \quad (47)$$

$$\mathbf{e}_h(t_k) = \mathbf{y}_h(t_k) - \hat{\mathbf{h}}_{\text{mle},i}(t_k). \quad (48)$$

For gyroscope measurements, also calculate

$$\mathbf{e}_{\dot{q}}^a(t_k) = \mathbf{y}_{\dot{q}}^a(t_k) - \hat{\mathbf{q}}_{\text{mle},i}^a(t_k). \quad (49)$$

For the case of distance meter form the error to be optimized as  $\mathbf{e}(t_k) = [\mathbf{e}_\tau^T(t_k), \mathbf{e}_h^T(t_k)]^T$ , and in the case of accelerometer and gyroscopes the error is formed as  $\mathbf{e}(t_k) = [\mathbf{e}_\tau^T(t_k), \mathbf{e}_h^T(t_k), \mathbf{e}_{\dot{q}}^a(t_k)]^T$ . Form the sum of squares to be minimized

$$S = \sum_{k=1}^{k=N} (\mathbf{e}(t_k)^T \boldsymbol{\Sigma}_{\tau,a}^{-1} \mathbf{e}(t_k)). \quad (50)$$

##### 3) Perform Gauss–Newton Update:

- a) Form the numerical gradient  $\mathbf{g}_{\text{mle}}$  of  $S$ .
- b) Form the numerical Hessian  $\mathbf{H}$  of  $S$ .
- c) Obtain the new ML estimate as

$$\mathbf{w} = \mathbf{H}^{-1} \mathbf{g}_{\text{mle}}. \quad (51)$$

- d) Increase iteration counter  $i$  by one and continue to step 2 or end if a stopping criterion of the optimization procedure is satisfied. Vector  $\mathbf{w} = \hat{\mathbf{h}}_{\text{mle},i,1\dots N}$  in the case of the distance meter and  $\mathbf{w} = [\hat{\mathbf{h}}_{\text{mle},i,1\dots N}^T, \hat{\mathbf{q}}_{\text{mle},i,1\dots N}^a]^T$  in the case of accelerometers.

The steps (3.a) to (3.d) are only illustrative and can be replaced by a particular implementation of nonlinear least squares minimization procedure.



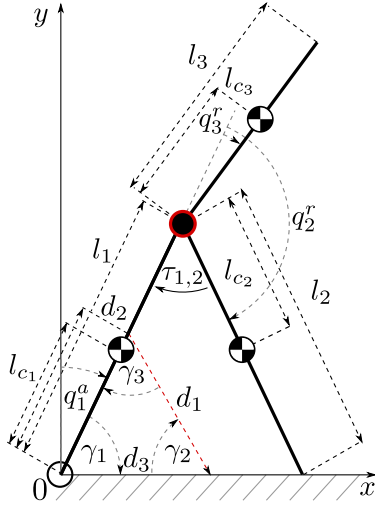


Fig. 2. Schematics of a 3-link robot.

### V. APPLICATION TO PARAMETER ESTIMATION OF A PLANAR BIPEDAL WALKING ROBOT

This section studies the simulation example of one of the simplest mechanical systems capable of underactuated planar bipedal walking [6], [13]. The robot is composed of three rigid links—two legs and a torso—connected by two actuated rotary joints. Schematics of robot are shown in Fig. 2. The set of configuration angles  $\mathbf{q}$  is composed of one absolute angle  $q_1^a$  and two relative angles  $q_2^r, q_3^r$ . It is assumed that the relative angles would be measured by incremental encoders and that the absolute orientation of the robot would be obtained by a laser distance sensor. The distance meter is rigidly fixed to the stance leg and is pointing toward the ground, see Fig. 2. Note that  $d_2$  denotes the distance from the point, where the stance leg touches the ground to the sensor location. Value of  $d_2$  is known and constant. The distance  $d_1$  is measured by the sensor. Furthermore, the angle  $\gamma_3$  between the stance leg and the optical axis of the sensor is also known and constant. The underactuated angle  $q_1^a$  can be obtained using equations

$$q_1^a = \frac{\pi}{2} - \arcsin\left(\frac{d_1}{d_3} \sin(\gamma_3)\right), \quad \text{for } d_1 \leq \frac{d_2}{\cos(\gamma_3)} \quad (52)$$

$$q_1^a = -\frac{\pi}{2} + \arcsin\left(\frac{d_1}{d_3} \sin(\gamma_3)\right), \quad \text{for } d_1 > \frac{d_2}{\cos(\gamma_3)} \quad (53)$$

where

$$d_3 = \sqrt{d_1^2 + d_2^2 - 2d_1d_2 \cos(\gamma_3)}. \quad (54)$$

Once the angle  $q_1^a$  is determined from the distance measurements  $d_1$ , the estimates for  $\dot{q}_1^a$  and  $\ddot{q}_1^a$  can be easily calculated using central differences. In this simulated study, the conversion from  $d_1$  to  $q_1^a$  was omitted for simplicity and it is assumed that directly  $q_1^a$  is measurable, thus the following measurement model was used both in the simulations and in the estimation procedure:

$$y_{q_1^a} = q_1^a + e_{q_1^a} \quad (55)$$

$$e_{q_1^a} \sim N(0, \sigma_{q_1^a}^2) \quad (56)$$

where the variance  $\sigma_{q_1^a}^2$  is known. Physical parameters of the robot are listed in Table I. Values of physical robot parameters

TABLE I  
PARAMETERS OF THE 3-LINK ROBOT

$l_1, l_2, l_3$	length of 1 <sup>st</sup> , 2 <sup>nd</sup> and 3 <sup>rd</sup> link	[m]
$l_{c1}, l_{c2}, l_{c3}$	center of gravity of 1 <sup>st</sup> , 2 <sup>nd</sup> and 3 <sup>rd</sup> link	[m]
$m_1, m_2, m_3$	mass of 1 <sup>st</sup> , 2 <sup>nd</sup> and 3 <sup>rd</sup> link	[kg]
$I_1, I_2, I_3$	inertia of 1 <sup>st</sup> , 2 <sup>nd</sup> and 3 <sup>rd</sup> link	[kg.m <sup>2</sup> ]
$\tau_1, \tau_2$	torque generated by 1 <sup>st</sup> and 2 <sup>nd</sup> motor	[N.m]
$g$	gravitational acceleration	[m.s <sup>-2</sup> ]

are based on a numerical example of [6] where a different parametrization is used. Parameters are as follows:

$$\begin{aligned} l_1 &= 1, \quad l_2 = 1, \quad l_3 = 0.5 \\ l_{c1} &= 0.5, \quad l_{c2} = 0.5, \quad l_{c3} = 0.2 \\ m_1 &= 5, \quad m_2 = 5, \quad m_3 = 25 \\ I_1 &= 0, \quad I_2 = 0, \quad I_3 = 1.5. \end{aligned} \quad (57)$$

Lagrangian formalism results in the following model matrices:

$$\begin{aligned} \mathbf{D} &= \begin{bmatrix} \beta_1 + \beta_2 + \beta_3 + 2\beta_4 c_2^r + 2\beta_5 c_3^r, & \beta_2 + \beta_4 c_2^r, & \beta_3 + \beta_5 c_3^r \\ \beta_2 + \beta_4 c_2^r, & \beta_2, & 0 \\ \beta_3 + \beta_5 c_3^r, & 0, & \beta_3 \end{bmatrix} \\ \mathbf{C} &= \begin{bmatrix} -\beta_4 \dot{q}_2^r s_2^r - \beta_5 \dot{q}_3^r s_3^r, & -\beta_4 s_2^r (\dot{q}_1^a + \dot{q}_2^r), & -\beta_5 s_3^r (\dot{q}_1^a + \dot{q}_3^r) \\ \beta_4 \dot{q}_1^a s_2^r, & 0, & 0 \\ \beta_5 \dot{q}_1^a s_3^r, & 0, & 0 \end{bmatrix} \\ \mathbf{G} &= \begin{bmatrix} -\beta_6 s_1^a - \beta_7 s_{1,2}^{a+r} - \beta_8 s_{1,3}^{a+r} \\ -\beta_7 s_{1,2}^{a+r} \\ -\beta_8 s_{1,3}^{a+r} \end{bmatrix}, \quad \mathbf{B} = \begin{bmatrix} 0 & 0 \\ 0 & -1 \\ 1 & 1 \end{bmatrix} \end{aligned}$$

using the following abbreviations:  $c_2^r = \cos(q_2^r)$ ,  $c_3^r = \cos(q_3^r)$ ,  $s_1^a = \sin(q_1^a)$ ,  $s_2^r = \sin(q_2^r)$ ,  $s_3^r = \sin(q_3^r)$ ,  $s_{1,2}^{a+r} = \sin(q_1^a + q_2^r)$ , and  $s_{1,3}^{a+r} = \sin(q_1^a + q_3^r)$ . Substitution

$$\begin{aligned} \beta_1 &= I_1 + l_1^2 m_2 + l_1^2 m_3 + l_{c1}^2 m_1, \quad \beta_2 = I_2 + m_2 l_{c2}^2 \\ \beta_3 &= I_3 + m_3 l_{c3}^2, \quad \beta_4 = l_1 l_{c2} m_2 \\ \beta_5 &= l_1 l_{c3} m_3, \quad \beta_6 = g(l_1 m_2 + l_1 m_3 + l_{c1} m_1) \\ \beta_7 &= g l_{c2} m_2, \quad \beta_8 = g l_{c3} m_3 \end{aligned} \quad (58)$$

makes the model linear with respect to the parameters  $\beta$ . The state space vector is given as

$$\mathbf{x} = (q_1^r, q_2^r, q_3^r, \dot{q}_1^a, \dot{q}_2^r, \dot{q}_3^r)^T. \quad (59)$$

#### A. Monte Carlo Analysis

Since the measurement of the absolute angle is corrupted with noise, a Monte Carlo simulations were utilized to analyze the performance of the estimation algorithms. Four cases with different variance  $\sigma_{q_1^a}^2$  were analyzed, see Table II. Furthermore, the case when  $\sigma_{q_1^a}^2 = 10^{-3}$  was also studied. In this case, the data begin to be too noisy with respect to their curvature and the resulting estimates ceases to be reliable due to premature termination of the optimization procedure. This case is used to demonstrate the effects of local minima. As a validation of proposed estimation method a  $10^3$  Monte Carlo simulations were performed for each setting of the variance  $\sigma_{q_1^a}^2$  totaling in  $4 \times 10^3$  simulations for the four cases described in Table II and additional  $10^3$  simulations were analyzed for the case when  $\sigma_{q_1^a}^2$  equals  $10^{-3}$ . The short duration of the

TABLE II  
FOUR STUDIED CASES AND MOST RELEVANT PARAMETERS

Simulation parameters	Case 1	Case 2	Case 3	Case 4
$\sigma_{q_1}^2$	$10^{-10}$	$10^{-8}$	$10^{-6}$	$10^{-4}$
$\sigma_{u_1}^2, \sigma_{u_2}^2$	$10^{-1}$	$10^{-1}$	$10^{-1}$	$10^{-1}$
Sampling Period $T_s$ [s]	0.01	0.01	0.01	0.01
Experiment Duration $T$ [s]	0.68	0.68	0.68	0.68
WLS-FCD parameters				
Half-power freq.	1	0.5	0.25	0.1
C.D. samples $n_{cd}$ [-]	2	3	5	7

experiments is due to the open-loop controller and the unstable nature of walking.

The MLE algorithm was compared with the WLS estimator based on the filtered central differences (FCDs). Filtering of the absolute angle measurements  $y_{q_1}^a$  was realized using MATLAB built in function `filtfilt`, which performs forward and backward filtering to reduce the distortion of data. The designed filter was a Butterworth filter of 5th order with a half power frequency, well-tuned for each  $\sigma_{q_1}^2$  separately according to Table II. The resulting filtered data are denoted as  $\hat{q}_{1,f}^a$ . Relative angular data  $q^r$  were not filtered, since they are available noise-free. The estimates of velocities and accelerations are calculated using central differences based on data  $\hat{q}_f = [q^{rT}, \hat{q}_f^a]^T$  as

$$\hat{q}_{fcd}(t_k) = \frac{\hat{q}_f(t_k + n_{cd}T_s) - \hat{q}_f(t_k - n_{cd}T_s)}{2n_{cd}T_s} \quad (60)$$

$$\hat{\dot{q}}_{fcd}(t_k) = \frac{\hat{q}_{fcd}(t_k + n_{cd}T_s) - \hat{q}_{fcd}(t_k - n_{cd}T_s)}{2n_{cd}T_s}. \quad (61)$$

Parameter  $n_{cd} \geq 1$  is related to the number of data samples used in the central-difference approximation of a derivative. Making the parameter  $n_{cd} > 1$  results in a smoother estimates of the derivatives for the specific values refer to Table II. This algorithm will be denoted as WLS with FCDs (WLS-FCDs). The MLE algorithm initial estimates of angles, angular velocities and accelerations are calculated using WLS-FCD algorithm. For comparison purposes the recursive least squares (RLS) and hybrid extended Kalman filter (HEKF) were tested as well. Their detailed implementation is provided in the appendix. The results of all estimation algorithms are summarized in Table III. By studying Table III, one can see that the performance of the MLE method is superior to all other approaches, especially for the cases, where the noise has larger variance. The RLS method, however, works also very well. The problem of HEKF lies in high nonlinearity of the system and, therefore, the filter is often unstable and fails to integrate.

## VI. PARAMETER ESTIMATION OF A LEG OF LABORATORY WALKING ROBOT

The aim of this section is to verify the proposed estimation procedure, described in Section IV, by estimating parameters of the leg of a prototype underactuated walking robot, which was firmly attached to a rigid platform. The identified system is shown in Fig. 3. The leg consists of two rigid links and two joints, the joint between the links is actuated, the other

TABLE III  
SAMPLE MEAN AND VARIANCE OF SUMMED SQUARED SIMULATION ERRORS OF THE 3-LINK ROBOT

MLE	Case 1	Case 2	Case 3	Case 4
Mean	1.242	1.231	1.195	1.149
Variance	0.009	0.010	0.011	2.567
Failed simulations	0	0	0	2
WLS-FCD	Case 1	Case 2	Case 3	Case 4
Mean	1.753	1.884	2.480	$6 \cdot 10^4$
Variance	0.016	0.055	5.023	$1.9 \cdot 10^{12}$
Failed simulations	0	0	0	132
HEKF	Case 1	Case 2	Case 3	Case 4
Mean	6.804	214.1	$10^3$	196.1
Variance	455.9	$10^7$	$2 \cdot 10^8$	$2.98 \cdot 10^6$
Failed simulations	25	228	246	160
RLS	Case 1	Case 2	Case 3	Case 4
Mean	1.245	0.5952	0.5136	7.1788
Variance	0.009	0.0279	0.1169	173.1557
Failed simulations	0	0	0	4



Fig. 3. Photograph of the prototype walking robot—front leg is identified.

joint is left intentionally unactuated and so it plays the role of the pivot. Therefore, only one motor is installed and the motor is equipped with an optical encoder to measure the relative angle  $q_2$  between the links. Furthermore, both joint angles  $q_1$  and  $q_2$  can be measured using a contactless hall encoders, which are used in order to provide benchmark measurements of both the actuated and the underactuated angle. However, these measurements are not used by the parameter estimation procedure. Therefore, this system possesses principal challenges that are characteristic for identification of underactuated walking robots. Finally, the motor torque  $\tau$  is measured using current shunt monitor and the leg is equipped with a 3-axis accelerometer—measuring proper acceleration  $a_x$  parallel with the leg link and  $a_y$  perpendicular to the upper link, both in the sagittal plane and  $a_z$  in the lateral plane—and a gyroscope—measuring angular velocity  $\dot{q}_1$ . The joint angle  $q_1$  is defined

TABLE IV  
PARAMETERS OF THE 2-LINK ROBOT LEG

$l_1, l_2$	length of 1 <sup>st</sup> and 2 <sup>nd</sup> link	[m]
$l_{c1}, l_{c2}$	center of gravity of 1 <sup>st</sup> and 2 <sup>nd</sup> link	[m]
$m_1, m_2$	mass of 1 <sup>st</sup> and 2 <sup>nd</sup> link	[kg]
$I_1, I_2$	inertia of 1 <sup>st</sup> and 2 <sup>nd</sup> link	[kg.m <sup>2</sup> ]
$\mu_1, \mu_2$	viscous friction parameters	[N.s/m]
$\mu_3, \mu_4$	Coulomb friction parameters	[N.s/m]
$g$	gravitational acceleration	[m.s <sup>-2</sup> ]

TABLE V  
SUMMED SQUARED ERRORS FOR IDENTIFIED MODEL OF  
THE ROBOT LEG SIMULATED ON VALIDATION DATA  
FROM REAL LABORATORY EXPERIMENT

Method	$\sum e_{q_1}^2$	$\sum e_{q_2}^2$	$\sum e_{\dot{q}_1}^2$	$\sum e_{\dot{q}_2}^2$
WLS-Hall	12.927	17.064	18.284	7.762
WLS-IMU	10.216	19.258	17.341	7.620
MLE-IMU	0.919	1.748	25.927	6.028

with respect to the horizontal axis passing through the center of the joint, parallel with the sagittal plane of the robot. Angle  $q_2$  is defined as a relative angle between the links. Corresponding physical parameters of the robot are listed in Table IV. A substitution rendering the model linear in parameters was used resulting in following matrices of the model:

$$\begin{aligned} \mathbf{D} &= \begin{bmatrix} \beta_1 + \beta_2 + 2\beta_3 \cos(q_2); & \beta_2 + \beta_3 \cos(q_2) \\ \beta_2 + \beta_3 \cos(q_2); & \beta_2 \end{bmatrix} \\ \mathbf{C} &= \begin{bmatrix} -2\beta_3 \sin(q_2)\dot{q}_2; & -\beta_3 \sin(q_2)\dot{q}_2 \\ \beta_3 \sin(q_2)\dot{q}_1; & 0 \end{bmatrix} \\ \mathbf{G} &= \begin{bmatrix} \beta_4 g \sin(q_1) + \beta_5 g \sin(q_1 + q_2) \\ \beta_5 g \sin(q_1 + q_2) \end{bmatrix} \\ \mathbf{F} &= \begin{bmatrix} \beta_6 \dot{q}_1 + \beta_8 \text{sign}(\dot{q}_1) \\ \beta_7 \dot{q}_2 + \beta_9 \text{sign}(\dot{q}_2) \end{bmatrix}, \quad \mathbf{B} = \begin{bmatrix} 0 \\ 1 \end{bmatrix}. \end{aligned} \quad (62)$$

The absolute orientation angle can be related with measurements using the accelerometer data  $a_x$ ,  $a_y$ , angular velocity  $\dot{q}_1$  measured by gyroscope and the angular acceleration  $\ddot{q}_1$ —which can be easily obtained by filtered differences from  $\dot{q}_1$ . These results in the following relation:

$$h = \begin{bmatrix} \sin(q_1) \\ \cos(q_1) \end{bmatrix} = \begin{bmatrix} \frac{l_s \ddot{q}_1 - a_{x,s}}{g} \\ \frac{-a_{y,s} - l_s \dot{q}_1^2}{g} \end{bmatrix}. \quad (63)$$

Since  $\sin(q_1 + q_2) = \sin(q_1)\cos(q_2) + \cos(q_1)\sin(q_2)$  and by combining with the optical incremental encoder measurements of the angle  $q_2$  and by approximating its derivatives  $\dot{q}_2$ ,  $\ddot{q}_2$  using FCDs, all the data required for constructing matrices  $\mathbf{D}$ ,  $\mathbf{C}$ ,  $\mathbf{G}$  are available. By using also the torque measurements it is possible to use the MLE method to estimate parameters  $\beta$ . Table V shows summed squared errors between response of simulated model obtained by identification and the real validation data—not the data set used for identification. Data were collected at sampling period of 0.01[s]. Three methods were compared, WLS method-based only on Hall sensor measurements for benchmark, then both WLS and MLE methods based on gyroscope and accelerometer data. We see

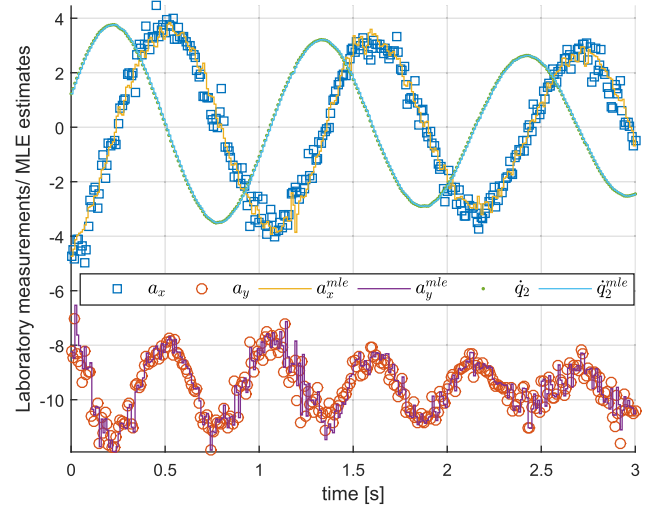


Fig. 4. Accelerometer and gyroscope measurements and their MLE estimates.

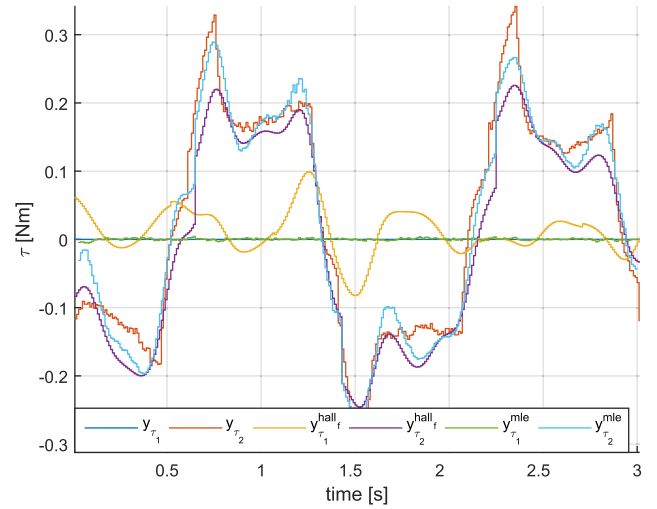


Fig. 5. Comparison of torques. Measured from current sensor, predicted by benchmark WLS model based on hall sensor measurements, predicted by the MLE based on accelerometer and gyroscope data.

that the MLE-based model is superior in predicting the angles  $q_1$  and  $q_2$ , which is exactly what is most important, even in comparison with the benchmark WLS method based on Hall measurements. The covariance matrices of data, which are required for algorithm to work, were tuned manually within several minutes. This further boost the practical usefulness of the algorithm. Fig. 4 shows ML estimates for accelerometer and gyroscope data - recall that data related to  $q_2$  are accurate and are not optimized. Fig. 5 shows torque prediction for benchmark model and the MLE model. Note especially excellent quality of the MLE prediction for the torque  $\tau_1$  on unactuated joint—which should be zero.

## VII. CONCLUSION

This brief analyzed the possible application of a novel identification method for walking robots based on ML method. Two cases were analyzed. First, a simulation example of a three link walking robot with a distance measurement was studied using Monte Carlo method. The second example was a real laboratory experiment focused on estimation of parameters of a leg of a walking robot using accelerometer

and gyroscope measurements. Both the simulations and the laboratory experiments provided very positive results. It can be concluded that the methods perform very favorably, even in comparison with other commonly used methods.

#### APPENDIX A

##### RECURSIVE LEAST SQUARES

The RLS can be implemented as follows [23].

- 1) *Initialization*: Initialize the parameter estimate  $\hat{\beta}(0)$  with some initial estimate, e.g., using WLS-FCD estimator. Initialize the covariance matrix  $\mathbf{P}(0)$  of the parameter estimate  $\hat{\beta}(0)$ .

- 2) *Estimation*: For  $t_k = 1 \dots N$ , perform following:

- a) Calculate the estimated torques using parameters  $\hat{\beta}(t_{k-1})$

$$\hat{\tau}(t_k) = \mathbf{Z}(\hat{\mathbf{q}}_{\text{fcd}}(t_k), \hat{\mathbf{q}}_{\text{fcd}}(t_k), \hat{\mathbf{q}}_{\text{fcd}}(t_k))\hat{\beta}(t_k). \quad (64)$$

- b) Calculate the gain matrix  $\mathbf{K}(t_k)$  and update the parameter estimates and the associated covariance matrix

$$\mathbf{K}(t_k) = \mathbf{P}(t_{k-1})\mathbf{Z}^T(t_k)(\mathbf{Z}(t_k)\mathbf{P}(t_{k-1})\mathbf{Z}(t_k) + \mathbf{R})^{-1} \quad (65)$$

$$\hat{\beta}(t_k) = \hat{\beta}(t_{k-1}) + \mathbf{K}(t_k)(\mathbf{y}_\tau(t_k) - \hat{\tau}(t_k)) \quad (66)$$

$$\mathbf{P}(t_k) = (\mathbf{I} - \mathbf{K}(t_k)\mathbf{Z}(t_k))\mathbf{P}(t_{k-1})(\mathbf{I} - \mathbf{K}(t_k)\mathbf{Z}(t_k)) + \mathbf{K}(t_k)\mathbf{R}(t_k)\mathbf{K}(t_k). \quad (67)$$

Matrix  $\mathbf{R} = \mathbf{B}\Sigma_u\mathbf{B}^T$  is of rank 2. Therefore, a regularization with some small number is necessary in order to prevent numerical instability of the algorithm.

#### APPENDIX B

##### HYBRID EXTENDED KALMAN FILTER

It is possible to estimate both states and parameters of the system (12) using HEKF [23]. Unknown robot parameters can be considered as state variables and the state vector can be augmented as

$$\bar{\mathbf{x}} = [\mathbf{x}^T, \boldsymbol{\beta}^T]^T. \quad (68)$$

Robot and measurement model are augmented as

$$\bar{\mathbf{x}} = \bar{\mathbf{f}}(\bar{\mathbf{x}}, \mathbf{u}, \mathbf{w}) = \begin{bmatrix} \mathbf{f}(\mathbf{x}) + \mathbf{g}(\mathbf{x})\mathbf{u} \\ \mathbf{0} \end{bmatrix} + \begin{bmatrix} \mathbf{w}_x \\ \mathbf{w}_\beta \end{bmatrix} \quad (69)$$

$$\mathbf{y}(t_k) = \bar{\mathbf{h}}(\bar{\mathbf{x}}(t_k), \mathbf{v}(t_k)). \quad (70)$$

Between the measurements the state vector is propagated according to augmented state equation and the covariance matrix of the estimation error is propagated according to

$$\dot{\mathbf{P}} = \mathbf{A}\mathbf{P} + \mathbf{P}\mathbf{A} + \mathbf{L}\mathbf{Q}\mathbf{L}^T \quad (71)$$

where

$$\mathbf{A} = \left. \frac{\partial \bar{\mathbf{f}}}{\partial \bar{\mathbf{x}}} \right|_{\hat{\mathbf{x}}^+(t_{k-1})}, \quad \mathbf{L} = \left. \frac{\partial \bar{\mathbf{f}}}{\partial \mathbf{w}} \right|_{\hat{\mathbf{x}}^+(t_{k-1})}.$$

The prior state estimate  $\mathbf{x}^-(t_k)$  and the prior covariance matrix estimate  $\mathbf{P}^-(t_k)$  are updated at each measurement time  $t_k$

$$\mathbf{K} = \mathbf{P}^-\mathbf{H}^T(\mathbf{H}\mathbf{P}^-\mathbf{H}^T + \mathbf{M}\mathbf{R}\mathbf{M}^T)^{-1} \quad (72)$$

$$\hat{\mathbf{x}}^+ = \hat{\mathbf{x}}^- + \mathbf{K}(\mathbf{y} - \bar{\mathbf{h}}(\hat{\mathbf{x}}^-)) \quad (73)$$

$$\mathbf{P}^+ = (\mathbf{I} - \mathbf{K}\mathbf{H})\mathbf{P}^-(\mathbf{I} - \mathbf{K}\mathbf{H})^T + \mathbf{K}\mathbf{M}\mathbf{R}\mathbf{M}^T\mathbf{K}^T \quad (74)$$

where we have dropped the time indices to save space

$$\mathbf{H}(t_k) = \left. \frac{\partial \mathbf{h}}{\partial \bar{\mathbf{x}}} \right|_{\hat{\mathbf{x}}^-(t_k)}, \quad \mathbf{M}(t_k) = \left. \frac{\partial \bar{\mathbf{h}}}{\partial \mathbf{v}} \right|_{\hat{\mathbf{x}}^-(t_k)}.$$

#### REFERENCES

- [1] B. Armstrong, "On finding 'exciting' trajectories for identification experiments involving systems with non-linear dynamics," in *Proc. IEEE Int. Conf. Robot. Autom.*, Mar. 1987, pp. 1131–1139.
- [2] A. Calanca, L. M. Capisani, A. Ferrara, and L. Magnani, "MIMO closed loop identification of an industrial robot," *IEEE Trans. Control Syst. Technol.*, vol. 19, no. 5, pp. 1214–1224, Sep. 2011.
- [3] M. Gautier, A. Janot, and P.-O. Vandanjon, "A new closed-loop output error method for parameter identification of robot dynamics," *IEEE Trans. Control Syst. Technol.*, vol. 21, no. 2, pp. 428–444, Mar. 2013.
- [4] M. Gautier and P. Poignet, "Extended Kalman filtering and weighted least squares dynamic identification of robot," *Control Eng. Pract.*, vol. 9, no. 12, pp. 1361–1372, 2001.
- [5] M. Gautier and P. Poignet, "Comparison of weighted least squares and extended Kalman filtering methods for dynamic identification of robots," in *Proc. IEEE Int. Conf. Robot. Autom. (ICRA)*, San Francisco, CA, USA, Apr. 2000, pp. 3622–3627.
- [6] J. W. Grizzle, G. Abba, and F. Plestan, "Asymptotically stable walking for biped robots: Analysis via systems with impulse effects," *IEEE Trans. Autom. Control*, vol. 46, no. 1, pp. 51–64, Jan. 2001.
- [7] A. Janot, P.-O. Vandanjon, and M. Gautier, "A generic instrumental variable approach for industrial robot identification," *IEEE Trans. Control Syst. Technol.*, vol. 22, no. 1, pp. 132–145, Jan. 2014.
- [8] A. Janot, P.-O. Vandanjon, and M. Gautier, "An instrumental variable approach for rigid industrial robots identification," *Control Eng. Pract.*, vol. 25, pp. 85–101, Apr. 2014.
- [9] A. Janot, M. Gautier, A. Jubien, and P.-O. Vandanjon, "Comparison between the CLOE method and the DIDIM method for robots identification," *IEEE Trans. Control Syst. Technol.*, vol. 22, no. 5, pp. 1935–1941, Sep. 2014.
- [10] H. K. Khalil, *Nonlinear Systems*. Englewood Cliffs, NJ, USA: Prentice-Hall, 2002.
- [11] L. D. Landau and E. M. Lifshitz, *Mechanics* (Course of Theoretical Physics), vol. 1, 3rd ed. New York, NY, USA: Elsevier, 1976.
- [12] L. Ljung, *System Identification: Theory for the User*. Hoboken, NJ, USA: Prentice-Hall, 1999.
- [13] T. McGeer, "Passive dynamic walking," *Int. J. Robot. Res.*, vol. 9, no. 2, pp. 62–82, Apr. 1990.
- [14] M. M. Olsen, O. J. Swevers, and W. Verdonck, "Maximum likelihood identification of a dynamic robot model: Implementation issues," *Int. J. Robot. Res.*, vol. 21, no. 2, pp. 89–96, 2002.
- [15] M. M. Olsen and H. G. Petersen, "A new method for estimating parameters of a dynamic robot model," *IEEE Trans. Robot. Autom.*, vol. 17, no. 1, pp. 95–100, Feb. 2001.
- [16] H.-W. Park, K. Sreenath, J. W. Hurst, and J. W. Grizzle, "Identification of a bipedal robot with a compliant drivetrain," *IEEE Control Syst. Mag.*, vol. 31, no. 2, pp. 63–88, Apr. 2011, doi: 10.1109/MCS.2010.939963.
- [17] J. Swevers, W. Verdonck, and J. D. Schutter, "Dynamic model identification for industrial robots," *IEEE Control Syst.*, vol. 27, no. 5, pp. 58–71, Oct. 2007.
- [18] J. Swevers, C. Ganseman, D. B. Tukel, J. de Schutter, and H. Van Brussel, "Optimal robot excitation and identification," *IEEE Trans. Robot. Autom.*, vol. 13, no. 5, pp. 730–740, Oct. 1997.
- [19] E. R. Westervelt, J. W. Grizzle, C. Chevallereau, J. H. Choi, and B. Morris, *Feedback Control of Dynamic Bipedal Robot Locomotion*. Boca Raton, FL, USA: CRC Press, 2007.
- [20] J. Wua, J. Wanga, and Z. You, "An overview of dynamic parameter identification of robots," *Robot. Comput. Integr. Manuf.*, vol. 26, no. 5, pp. 414–419, 2010.
- [21] N. L. El Yaaqoubi and G. Abba, "Identification of physical parameters including ground model parameters of walking robot rabbit," in *Proc. 9th IEEE-RAS Int. Conf. Humanoid Robots*, Paris, France, Dec. 2009, pp. 269–276.
- [22] *Inemo Inertial Module: 3D Accelerometer, 3D Gyroscope, 3D Magnetometer, LSM9DS1, Rev 3*, STMicroelectronics, Geneva, Switzerland, Mar. 2015.
- [23] D. Simon, *Optimal State Estimation*. Hoboken, NJ, USA: Wiley, 2006.